coatings

MDPI

Article

Survey of Indigenous Bacteria as a Simplified Alternative to Produce Self-Healing Cementitious Matrices

Vinicius Muller [1], Henrique dos Santos Kramer [1], Fernanda Pacheco [1], Hinoel Zamis Ehrenring [1], Roberto Christ [2], Victor Valiati [3], Regina Célia Espinosa Modolo [4] and Bernardo Fonseca Tutikian [1,*]

[1] Itt Performance—Technical Institute in Performance and Civil Construction, UNISINOS University, São Leopoldo 93022-750, Brazil; vmullerm1@gmail.com (V.M.); henriquekramer@edu.unisinos.br (H.d.S.K.); fernandapache@unisinos.br (F.P.); hzamis@unisinos.br (H.Z.E.)
[2] Civil and Environmental Engineering Department, Universidad de la Costa, Calle 58 #55-66, Barranquilla 080002, Colombia; rchrist@unisinos.br
[3] Biology Department, UNISINOS University, São Leopoldo 93022-750, Brazil; valiati@unisinos.br
[4] Civil Engineering and Mechanical Engineering Department, UNISINOS University, São Leopoldo 93022-750, Brazil; reginaem@unisinos.br
* Correspondence: bftutikian@unisinos.br

Abstract: The cracks in concrete serve as pathways for aggressive agents, leading to deterioration. One approach to addressing these cracks and enhancing structures durability is the use of self-healing agents, such as bacteria used to heal cracks in cementitious matrices. Bacteria can be found in several environments, and their identification and healing viability must be evaluated prior to their use in cementitious matrices. In this study, distinct indigenous bacteria were collected from soil in industrial yards associated with the cement industry. These bacteria were identified and incorporated in cement and mortar mixtures with 18% entrained air. X-ray diffraction (XRD) and scanning electron microscopy (SEM) analyses were performed to characterize the formed products, and compressive strength testing was conducted to evaluate the mechanical properties of the mortars. The identified bacteria were of the genus *Cronobacter*, *Citrobacter*, *Bacillus*, and *Pseudomonas*, and their potential to form self-healing products was evaluated with microscopic and mineral analyses. Results showed that all bacteria could form calcite ($CaCO_3$) crystals, with full crack healing in some of the samples. Mechanical testing indicated increases in average compressive strength of up to 108% at 28 days with respect to a reference mortar.

Keywords: self-healing; bacteria; indigenous; entrained air; durability; cement matrix

Academic Editor: Qiao Dong

Received: 28 November 2024
Revised: 23 January 2025
Accepted: 24 January 2025
Published: 30 January 2025

Citation: Muller, V.; Kramer, H.d.S.; Pacheco, F.; Ehrenring, H.Z.; Christ, R.; Valiati, V.; Modolo, R.C.E.; Fonseca Tutikian, B. Survey of Indigenous Bacteria as a Simplified Alternative to Produce Self-Healing Cementitious Matrices. *Coatings* **2025**, *15*, 152. https://doi.org/10.3390/coatings15020152

1. Introduction

Cracking is a harmful natural process in reinforced concrete due to the limited tensile strength of the material [1]. Cracks allow the ingress of aggressive agents, which damage the material and decreases its durability [2–4]. Since concrete consumption has a considerable environmental impact and its production accounts for 5% to 7% of global CO_2 emissions [5], there is a direct benefit in developing methodologies that increase the durability of cementitious matrices.

Over the past few years, several techniques for repairing cracks have been developed, but these have been expensive and in most cases temporary [6]. These techniques could also require constant inspection, which would prevent their application

in large structures or buildings with a lack of access points [1,7]. Thus, self-healing has been noted as a potential sustainable recovery method for cementitious composites [6], as it has the potential to act from crack formation and its application would not require direct manual intervention [1].

Concrete alone is a material with self-healing potential since, over time, hydration of anhydrous cement grains or carbonation of calcium hydroxide ($Ca(OH)_2$) can fill in void spaces and cracks [8]. This autogenous self-healing is limited to small cracks up to 0.1 mm in size [9] and is difficult to control with precision since it requires the presence of water. It also has limited scope since it relies on the availability of reactive materials in the cementitious matrix [8]. Autonomous self-healing is another option, in which specific materials with the ability to seal cracks are added to the matrix. The use of bacteria is one of the most promising such techniques with the additional benefit of decreasing environmental impact [10–12]. Bacteria incorporated in concrete can form calcium carbonate ($CaCO_3$) up to four times more efficiently than the hydration of anhydrous cement for the purposes of filling void spaces and cracks [9,13,14]. This is known as microbially induced calcium carbonate precipitation (MICP), and its filler effect on void spaces [10] also produced decreased porosity by over 50% [15] and increased compressive strength by 42% [16].

Bacteria can utilize two metabolic processes in the generation of $CaCO_3$: heterotrophic and autotrophic processes [17]. The heterotrophic process is mostly used by bacteria and other microorganisms for $CaCO_3$ production [18]. In this process, bacteria can perform urease hydrolysis [4,17,19–21], denitrification, ammonification, and dissimilatory sulfate reduction [21,22]. The autotrophic process, on the other hand, is carried out by microorganisms that use photosynthesis [17,18,21,22].

Most studies make use of bacteria from known databases [12,23–25] or from commercial enterprises that offer materials for the production of self-healing concretes [26]. However, a few studies have evaluated indigenous bacteria as self-healing agents [15,27–30]. Indigenous bacteria are native microorganisms from the location where the studies are conducted, which are collected, isolated, and identified. The use of indigenous bacteria from locations in contact with Portland cement may be a viable approach, as these microorganisms are adapted to an environment with chemical characteristics similar to those of the cementitious matrix [31,32]. This methodology increases the number of known bacteria suitable for use in self-healing concretes and allows the prospection of local bacteria. This produces economic and sustainable benefits and promotes the use of bio-concretes.

Other studies have stated that the high compaction, alkaline pH, and low oxygen content of cementitious matrices create an unfavorable environment for the survival of bacteria, which, consequently, would require some form of encapsulation [31,32]. Common encapsulation techniques that could be used include light aggregates [33,34], fibers [16,34–36], and iron oxide microparticulates [37]. While efficient, such techniques required advanced equipment, which limited their large-scale viability [38]. Alternatively, studies have shown that bacterial solutions incorporated into air-entraining admixtures were delivered efficiently. Air microbubbles, with diameters ranging from 0.02 to 1 mm, can assist spore survival due to the available space [39,40]. It was observed [24] that the bacteria became encapsulated within the air bubbles, resulting in up to an 18% reduction in mortar water permeability.

Thus, the objective of this study was to address the gap in knowledge regarding self-healing cementitious matrices by exploring the use of indigenous bacteria. These bacteria, naturally occurring in soil from industrial yards with Portland cement residues, were identified, isolated, and incorporated into a cementitious matrix. An air-entraining

admixture was employed as an encapsulating agent to enhance the performance of the matrix.

2. Materials and Methods

The experimental program was conducted in four stages: soil collection and selection and identification of bacteria; reproduction of the selected bacteria; preparation of the samples; and microstructural and mechanical analysis of the mortars. The entirety of the experimental study is summarized in the flowchart of Figure 1.

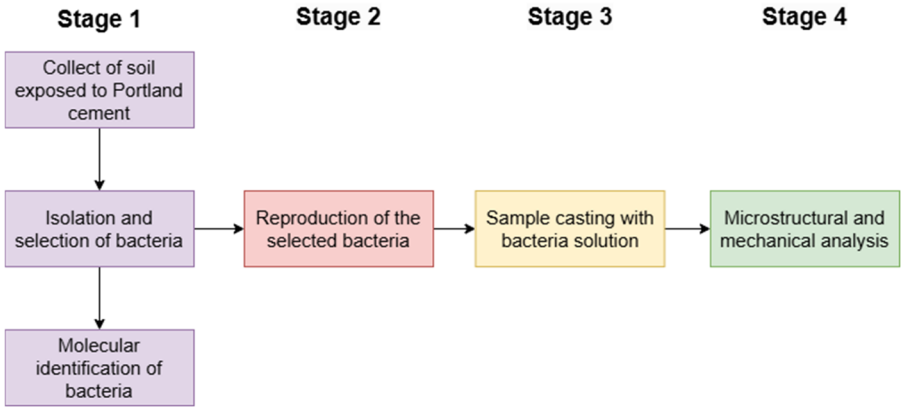

Figure 1. Flowchart of the experimental study.

2.1. Materials

The binder used in this study was high early strength (HE) Portland cement as defined by standard ASTM C150:2022 [41]. This type of cement was used because it does not contain pozzolanic materials, preventing autonomous self-healing through pozzolanic reactions. Bacteria were selected from soil exposed to Portland cement and followed the procedure of Section 2.3. For protection, bacteria were encapsulated in the air-entraining admixture Centrament Air 200® manufactured by MC-Bauchemie (Bottrop, Germany). The amount of admixture added was set as the intermediate value between the minimum content (0.20% relative to the cement mass) and the maximum content (0.50% relative to the cement mass), as recommended by the manufacturer. The admixture was added to the bacteria solution before the mixture. The aggregate was quartz pit sand, the most common type in the region where this study was conducted.

The cement and aggregate physical properties are shown in Table 1. The chemical composition of cement is shown in Table 2.

Table 1. Physical properties of cement and aggregate.

Material	Property		
Sand	Dry specific mass		2.56 g/cm³
	Maximum characteristic size		4.75 mm
	Fineness modulus		3.49
Cement	Blaine specific surface		4400 cm²/g
	Fineness (#200)		0.08%
	Fineness (#325)		0.40%
	Setting time	Initial	160 min
		Final	210 min
	Water content for normal consistency paste		29.1%
	Mechanical compressive strength	1 day	26.3 MPa
		3 days	39.4 MPa
		7 days	45.7 MPa
		28 days	53.4 MPa

Table 2. Chemical composition of cement used in this study.

Compound	Mass Fraction (%)
Al_2O_3	4.44
SiO_2	18.52
Fe_2O_3	3.14
CaO	61.05
MgO	3.64
SO_3	2.85
Loss on ignition (LOI)	3.19
Free CaO	1.99
Insoluble residue	1.01
Equivalent alkali content	0.62

2.2. Mix Ratio

The mix ratio was based on previous studies [42,43] and properly adjusted to the entrained air content needed to protect the bacteria. The mix ratio is shown in Table 3.

Table 3. Mix ratio with respect to mass for production of mortars.

Cement	Sand	Water [1]/Cement (w/c)	Air-Entraining Admixture (with Respect to Mass of Cement)	Entrained Air Content [2]	Cement Consumption
1.0	1.0	0.4	0.35	18%	709.9 kg/m^3

[1] All water was replaced with bacterial solution. [2] Determined from the methodology of standard ABNT NBR 16887, 2020 [44].

2.3. Bacteria Survey

The bacteria selection procedure was based on a previous study [45] and consisted of isolating samples from soil. More specifically, samples were collected from soils already exposed to cement, which increased the likelihood that the bacteria had a degree of resistance to some of the chemical conditions found within the cementitious matrix [31,32]. Five samples were collected from two types of soil (A and B) in industrial yards that were in contact with Portland cement. Soil type A was sandy and was collected from around a cement silo in a prefabricated element concrete plant yard in Porto Alegre/Brazil. Soil type B was clayish and was collected from around a coarse aggregate stack in a concrete plant in Novo Hamburgo/Brazil. In all cases, samples were collected from a drilling depth of 5 cm. Each drill hole was designated in accordance to soil type and numbered in sequential order, as shown in Figure 2.

(**a**) (**b**)

Figure 2. Sample collection from soil types (**a**) A and (**b**) B.

Following collection, a 2 g portion of each sample was individually suspended in 25 mL of calcium lactate solution at 37 °C for 24 h to promote bacterial growth. The calcium lactate solution was taken from previous studies [42,46] in which it had demonstrated positive results and allowed bacteria selection. It consisted of deionized water with contents of 8 g/L of calcium lactate and 1 g/L of yeast extract. Streak plating was used to isolate the bacteria with a calcium lactate agar medium with the same composition as the solution but with the addition of 16 g/L of agar. Plates were incubated at 37 °C for 24 h and visually inspected to determine colonial morphology [27]. Subsequent and repetitive streakings were conducted until isolated colonies were obtained.

After isolating the colonies, bacteria identification and morphological analysis were conducted [47]. These consisted of catalase, motility, urease, oxidation, fermentation, bile esculin, TSI, and citrate tests followed by separation of thick-cell-wall bacteria with Gram staining [48]. Bacteria with equal results in biochemical and Gram staining had their duplicates discarded. Selected bacteria had their DNA extracted with the salting-out method following Wizard Genomic DNA Purification Kit® (Madison, WI, USA) Promega protocol. The concentration and quality of the genome DNA were estimated with Nanodrop™ UV–VIS spectrophotometry (Thermo Scientific™, Wilmington, DE, EUA). Products from DNA extraction were used to amplify the region of gene 16S rRNA in a segment of approximately 1200 pb with a PCR technique and primer forward 27F (5′ AGAGTTTGATCCTGGCTCAG 3′), primer reverse MHR1 (5′ CCTTGTTACGACTTCACCC 3′), and added cytokine (C) at position 5′ [49]. The PCR sample was composed of 1 μL extracted DNA, 4 μL Master Mix Fire Pool (Ludwig Biotech Ltd.a.) reagent solution, 1 μL primer forward, 1 μL primer reverse, and 13 μL ultrapure water. Amplification was conducted with a thermocycler operating with the following conditions: initial denaturation (4 min at 94 °C), 38 denaturation cycles (1 min each at 94 °C), annealing (40 s at 55 °C), extension/elongation (90 s at 72 °C), and final elongation (5 min at 72 °C).

Amplicon quantification was conducted with Nanodrop™ UV–VIS spectrophotometry (Thermo Scientific™, Wilmington, DE, USA). PCR verification was performed with electrophoresis (45 min at 90 V) in a 1% agarose gel with GelRed (Biotium, Hayward, CA, USA) nucleic acid fluorescent dye and 100 bp DNA Ladder Invitrogen™ base pair size marker after amplification. Results were visualized under UV light with a transluminator. Purification made use of Shrimp Alkaline Phosphatase (SAP) and exonuclease with Exo I enzyme (New England Biolabs, Ipswich, MA, USA) with a ratio of 0.3 μL of Exo I enzyme and 0.8 μL of SAP enzyme for each 10 μL of PCR product. The procedure was conducted for 20 s at 37 °C, 15 min at 85 °C, and kept at 12 °C until removal from the thermocycler. Sequencing was conducted by Advancing Enterprise through Genomics MACROGEN in the Republic of South Korea. Each sample was sequenced in both sense and antisense directions.

For each isolated sequence, consensus was obtained from sense and antisense strands with Staden Package 2.0 open-source software (http://staden.sourceforge.net/). Sequence reliability was evaluated visually with a complete chromatogram obtained from ChromasPro commercial software (http://www.technelysium.com.au). A five-sequence consensus was generated and automatically aligned on ClustalW program running MEGA 7 software [50] and post-edited on BioEdit 5.0.9 freeware [51]. After alignment, each 16S rRNA gene sequence was used as a query in comparison with sequences available in NCBI Genbank with BLAST tool. In all cases, BLAST produced matching 16S rRNA sequences with good coverage (≥80%) and identification (>98%) and suggested that nucleotide sequences from soil samples corresponded to the 16S region of the bacterial genome.

2.4. Sample Production

Isolated bacteria were inoculated separately in calcium lactate solution. The inoculums were cultivated in a shaker kept at 165 rpm and 37 °C, for 24 h [42]. The cultivated bacterial solution was used as a replacement for water in the mortar mixture without further dilution or micro-organism count [43,44].

Mixing was performed in a mechanical mixer and followed the procedures of standard ABNT NBR 7215:2019 [52]. Cement and all calcium lactate solutions were mixed for 30 s at 140 rpm ± 5 rpm. Fine aggregate was gradually added over 30 s, and the materials further mixed for 30 s at 285 ± 10 rpm. The mixer was turned off, and the mortar allowed to rest for 1 min 30 s, followed by one further mixing of 1 min at 285 rpm ± 10 rpm. Test bodies of cylindrical and prismatic shapes were then molded for each bacteria sample as shown in Table 4. It is emphasized that, as this study used a mix ratio applied in other studies [42], a reference mortar without bacteria was not used for visual verification.

After molding, test bodies were kept in a controlled environment at 23 °C ± 2 °C and relative humidity above 95%.

Table 4. Dimensions and characteristics of test bodies of this study.

Shape	Dimensions	Number of Test Bodies per Bacteria	Analysis Conducted on Test Body
Prismatic [1]	4 cm × 4 cm × 16 cm	3	Visual analysis of self-healing and X-ray diffraction (XRD)
Cylindrical [2]	5 cm × 10 cm	1	Scanning electron microscopy (SEM)
Cylindrical [2]	5 cm × 10 cm	6	Compressive strength

[1] Molded in accordance with standard NBR 13279:2005 [53] with a CA 60 steel bar 5 mm in diameter positioned as reinforcement to control the amount of cracking. [2] Molded in accordance with standard NBR 7215:2019 [52].

2.5. Cracking and Self-Healing

Self-healing was tested on prismatic test bodies 7 days after molding. Cracks were mechanically induced by a three-point flexural test with a load of 100 N/s until at least one crack was visible. For the cylindrical test bodies, a smaller cylinder measuring 2 cm × 3 cm was extracted from one of each sample at 7 days for microstructural evaluation of self-healing. The smaller cylindrical test body was subjected to diametric compression to induce cracking. To prevent fragmentation, the entire test body was wrapped in adhesive tape as per previous studies [54]. The remaining original cylindrical test bodies were used for compressive strength tests and were not subjected to cracking.

Following cracking, all test bodies were stored in a controlled environment at 23 °C ± 2 °C and relative humidity above 95% until reaching the assigned age for analysis. The conditions for self-healing were the same as in other studies [55] and assumed that bacteria within the cementitious matrix would be in contact with both oxygen and water, which would promote their metabolism and increase healing capacity as shown previously [56]. To this end, the prismatic test bodies were acclimated with the crack facing up to further promote contact with oxygen and humidity. This also removed variations in calcium carbonate ($CaCO_3$) deposition due to crack placement.

2.6. Post-Healing Evaluation

Crack sealing was monitored with an optical microscope. A large crack was identified in each prismatic test body and inspected at 0 days, 7 days, 14 days, and 28 days after cracking.

The morphology of the healing compounds formed in the cracks was determined with scanning electronic microscopy (SEM) on the small cylinder samples. Cracked samples were kept in the controlled environment for 28 days and dried in an oven at 40 °C for 7 days. The adhesive tape was removed, and the two halves formed from the diametric compression separated. The internal surface of the cracks was metalized with gold and analyzed with a Zeiss SEM model EVO MA 15 with an acceleration of 15 kV.

The mineral composition of healing products was evaluated with X-ray diffraction (XRD). Healing material was collected with a sterilized needle after 28 days in storage. The XRD apparatus was a PANanalytical brand Empyrean model with interval angle from 5° to 75°, time of 1 s, and step of 0.05. The effect of bacteria on compressive strength was evaluated at 7 days and 28 days on cylindrical test bodies as recommended by standard ABNT NBR 7215:2019 [52].

3. Results and Discussion

3.1. Bacterial Survey

All collected soil samples contained bacteria capable of growth in calcium lactate medium. Following isolation, 10 distinct bacteria were found for analysis. Biochemical tests and duplicates decreased the bacteria to five isolated bacterium (IB) samples for use in the cementitious matrix. Molecular identification up to the genus level and collection location are shown in Table 5. Specific determination of the five bacteria was not possible due to the high genetic similarity between species of each genus.

Table 5. Molecular identification of selected and isolated bacteria.

Bacteria	Soil	Phylum	Class	Order	Family	Genus
IB1	A-II	*Proteocteria*	*Gammaproteocteria*	*Enterobacterales*	*Enterobacteriaceae*	*Cronobacter*
IB2	A-V	*Proteocteria*	*Gammaproteocteria*	*Enterobacterales*	*Enterobacteriaceae*	*Cronobacter*
IB3	B-I	*Firmicutes*	*Bacilli*	*Bacillales*	*Bacillaceae*	*Bacillus*
IB4	B-II	*Proteocteria*	*Gammaproteocteria*	*Enterobacterales*	*Enterobacteriaceae*	*Citrobacter*
IB5	B-IV	*Proteocteria*	*Gammaproteocteria*	*Pseudomonadales*	*Pseudomonadaceae*	*Pseudomonas*

Regarding the identified isolated genera, *Bacillus* (IB3) is known to have several species of bacteria able to produce spores with resistant and adequate structure for use in cementitious matrices [31,57]. Consequently, it has already been used in several self-healing studies of concretes and mortars [37,42,46,55,58–61]. On the other hand, *Pseudomonas* (IB5) is a genus found in humid conditions [62], and its diverse metabolisms have allowed it to be used in several different environments [48]. *Pseudomonas* metabolism is classified as chemoorganotrophic with several sources of carbon for nutrition, which allowed it to thrive in a calcium lactate solution [63]. Similar to *Bacillus*, *Pseudomonas* has been used for the self-healing of cracks in cementitious matrices [64,65].

The genera *Cronobacter* (IB1 and IB2) and *Citrobacter* (IB4) are both from the *Enterobacteriaceae* family. This family is commonly found in the intestinal tract of humans and other animals, and some species are linked to infections [66,67]. These genera had less potential for self-healing, and their presence in the collected soil samples were likely a result of contamination from animal urine and feces [68]. *Enterobacteriaceae* metabolism is cited as glucose conversion into acid or acid conversion into gas, such as nitrate into nitrite [67]. Some studies were able to isolate several bacteria that could precipitate calcium carbonate ($CaCO_3$) from an organic source of calcium (calcium acetate) such as *Salmonella*. Thus, it was possible for *Enterobacteriaceae* to grow with calcium lactate as a source of carbon, and, as such, *Citrobacter* and *Cronobacter* were selected for self-healing in this study

3.2. Crack Sealing

Figure 3 shows cracks and self-healing progression from test bodies incorporating IB1 and IB2 *Cronobacter* spp. isolated from Soil A.

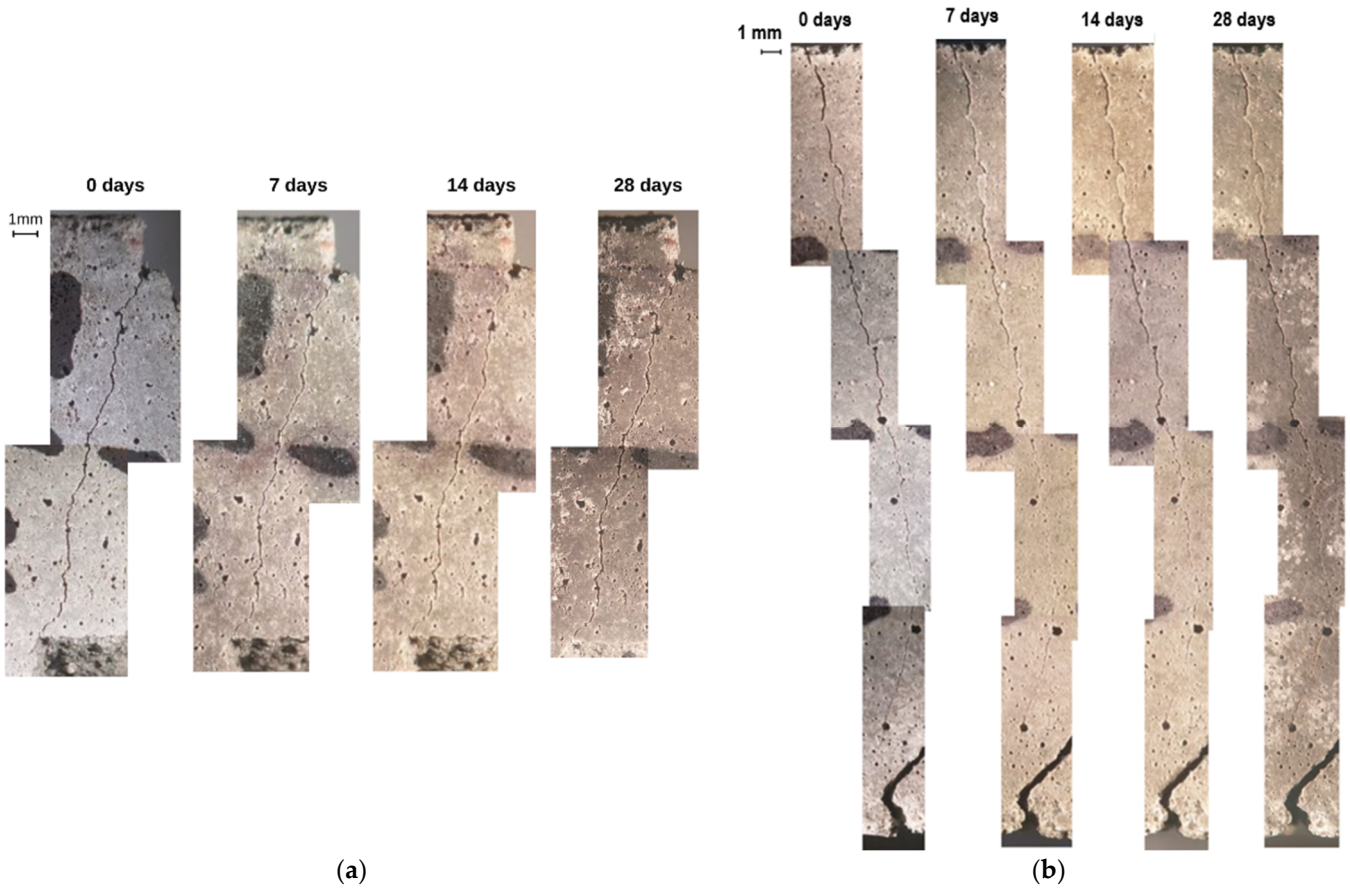

Figure 3. Crack healing progression on test bodies at 0 days, 7 days, 14 days, and 28 days of age with Soil A bacteria (**a**) IB1 *Cronobacter* sp. and (**b**) IB2 *Cronobacter* sp.

Figure 3 shows that no crack was sealed throughout the time periods of this study. However, crystals were found on other test body faces not assigned for analysis. Figure 4 shows healing products formed on a crack on the side face of a test body incorporating IB2 *Cronobacter* sp. over the same ages. Crystals could be seen on the crack at 7 days of age and increased in quantity at 14 days. However, the amount of crystals decreased at 28 days, demonstrating a partial loss of healing products. Reductions in healing products over time were observed in previous studies and were attributed to their composition, crack characteristics, and presence of water [55]. The healing product observed in Figure 4 had white coloration, a possible indicative of calcium carbonate ($CaCO_3$) [69], and matched the results of other studies [55,58].

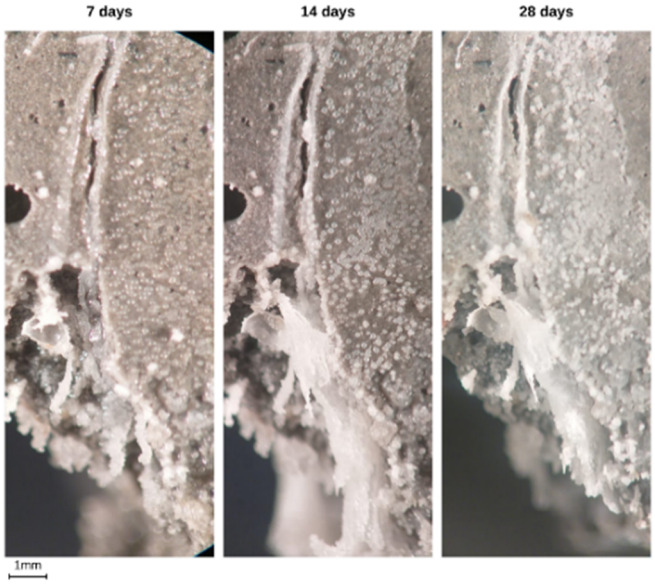

Figure 4. Healing product formation on the side face of a test body incorporating IB2 *Cronobacter* sp. at 7 days, 14 days, and 28 days.

It should be noted that all prismatic test bodies were stored in the same orientation, with the main crack facing up, and a pattern emerged of healing products appearing in the lower part of the prisms. Furthermore, results from SEM and XRD confirmed calcium carbonate formation in all test bodies. Thus, it was possible that calcium carbonate formed from MICP on the top face crack before 7 days of age but lacked adhesiveness to the cementitious matrix. Consequently, it was hypothesized that water condensation on the top face crack could have percolated from gravity and carried and deposited crystals at the lower part of the prisms. Other studies [70] have demonstrated that calcium carbonate as calcite had higher adhesiveness to cement hydrates than aragonite. Thus, it was also possible that crystal structure also influenced the stability of healing products inside the cracks. Another possibility would be calcium carbonate solubility in percolating water, which would carry crystals to the lower part of the prism and eventually out of the test body. However, this was an unlikely scenario since most studies considered calcium carbonate to have low water solubility [69].

Figure 5 shows cracks and self-healing progression from test bodies incorporating bacteria IB3 *Bacillus* sp., IB4 *Citrobacter* sp., and IB5 *Pseudomonas* sp. from Soil B.

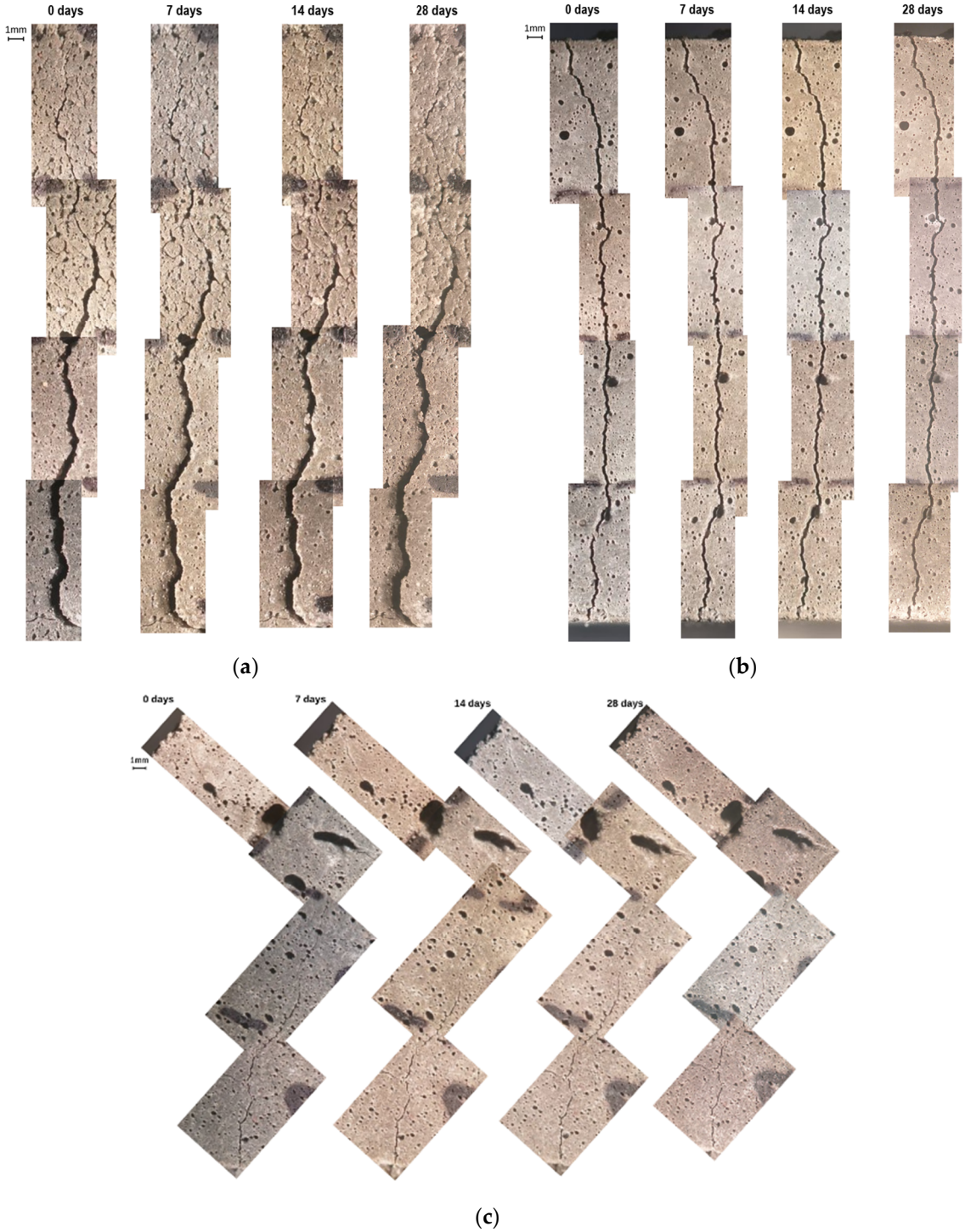

Figure 5. Crack healing progression on test bodies at 0 days, 7 days, 14 days, and 28 days of age with Soil B bacteria (**a**) IB3 *Bacillus* sp., (**b**) IB4 *Citrobacter* sp., and (**c**) IB5 *Pseudomonas* sp.

As for test bodies incorporating Soil A *Cronobacter* spp. bacteria, no healing products were noted in the top face cracks, but white healing products, likely calcium carbonate, were found on the lateral faces and lower portions of the samples. Figure 6 shows one of the IB3 *Bacillus* sp. test bodies where white crystals were observed on the lateral face at 14 days and increased over time to completely fill the crack at 28 days. Similarly, Figure 7 shows healing products on the bottom face of a test body incorporating IB4 *Citrobacter* sp., while Figure 8 shows localized crystals in the cracked face of a test body incorporating IB5 *Pseudomonas* sp. Since the location and formation of healing products on mortars

incorporating Soil B bacteria were equivalent to the ones with Soil A, the same proposed explanations of their occurrence could also be surmised.

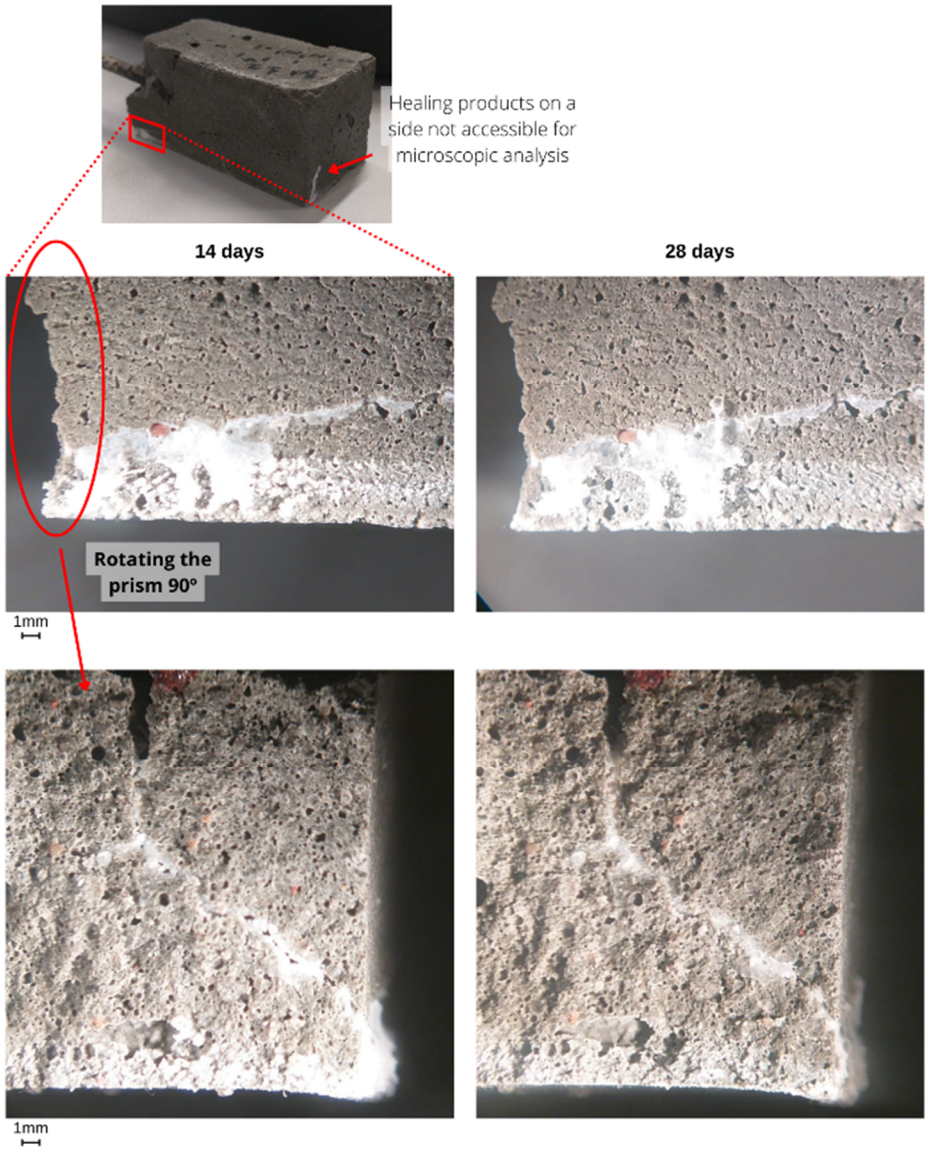

Figure 6. Crack healing on the lateral face of a test body incorporating IB3 *Bacillus* sp. at 14 days and 28 days.

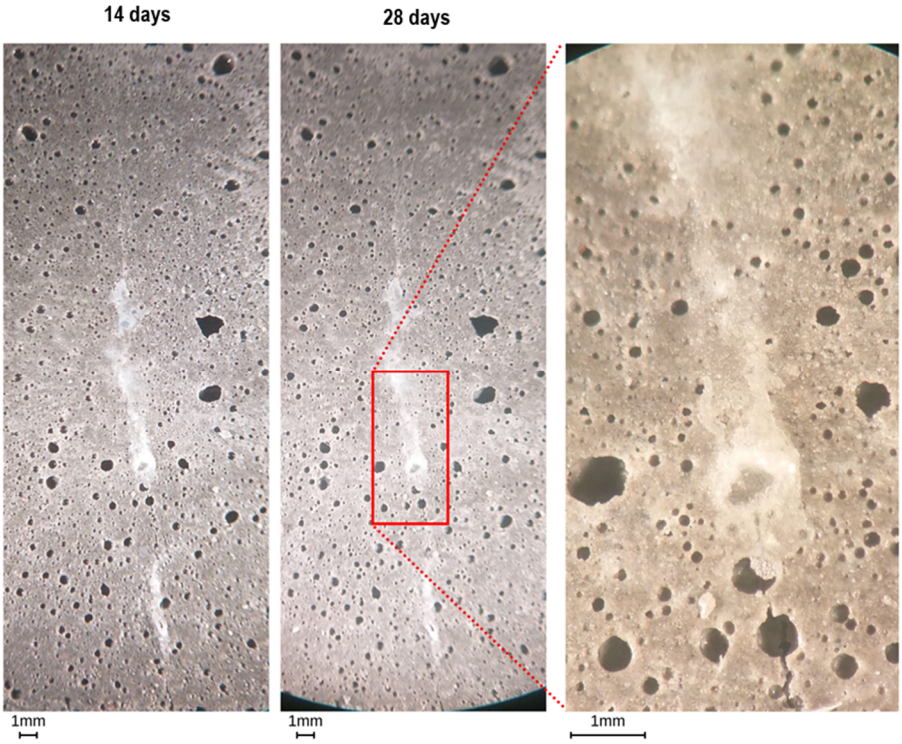

Figure 7. Crack healing on the bottom face of a test body incorporating IB4 *Citrobacter* sp. at 14 days and 28 days.

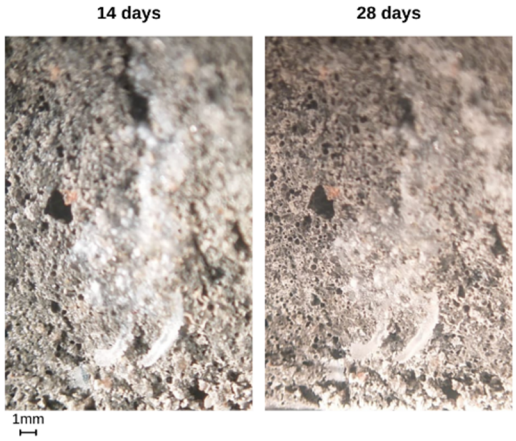

Figure 8. Localized healing crystal formation on a test body incorporating IB5 *Pseudomonas* sp. at 14 days and 28 days.

3.3. Morphology and Mineral Composition of Healing Products

Figures 9a–13a show the exposed crack surface of test bodies with IB1 *Cronobacter* sp. Images were obtained from the separation of the two halves of the fractured small cylindrical prism. The exposed crack surface was white in color, and the whitest spots identified visually (indicated by the black arrows in the figures) were selected for SEM analysis to verify the morphology of the formed products, with selected images shown in Figures 9b–13b.

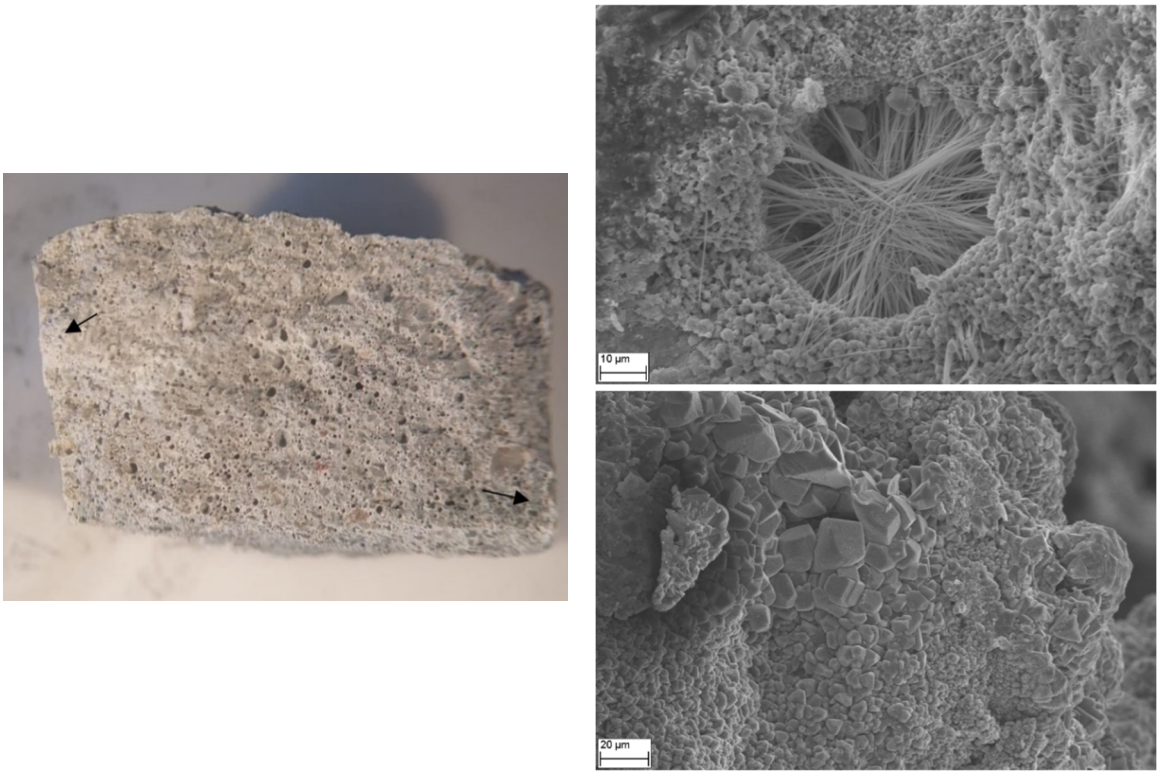

(**a**) (**b**)

Figure 9. (**a**) Exposed crack face of test body with IB1 *Cronobacter* sp. and (**b**) SEM image of selected locations marked with black arrows.

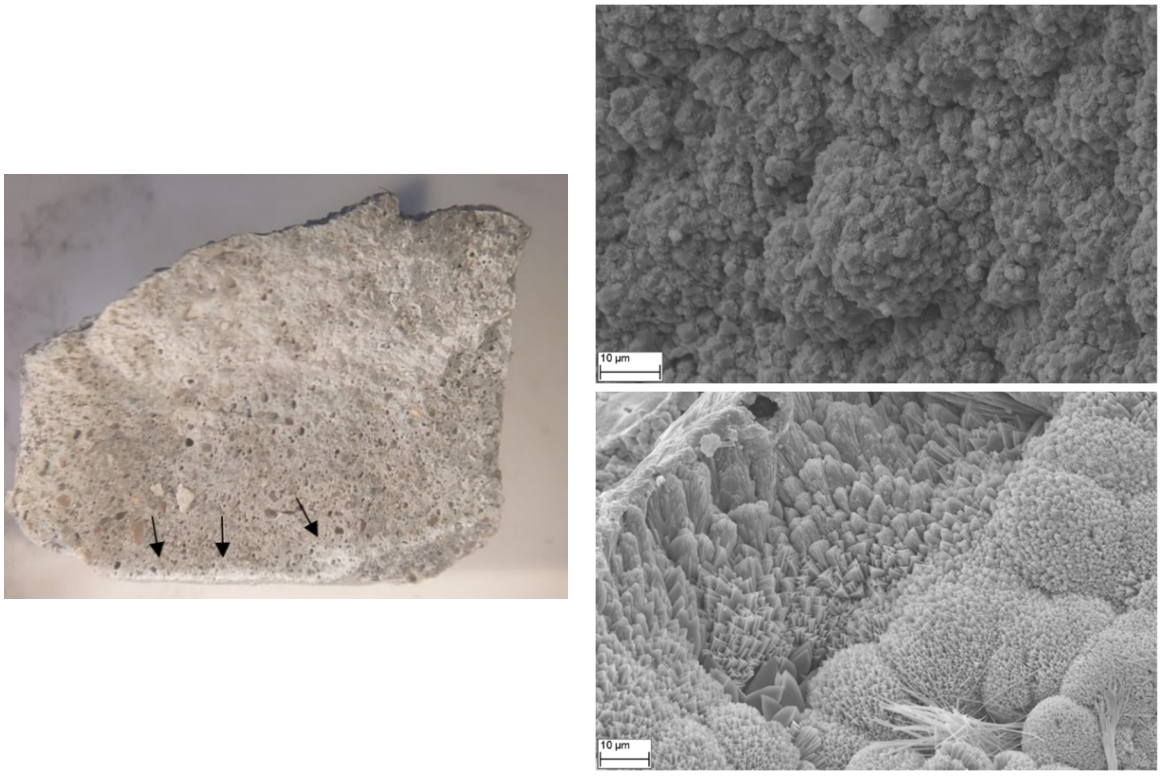

(**a**) (**b**)

Figure 10. (**a**) Exposed crack face of test body with IB2 *Cronobacter* sp. and (**b**) SEM image of selected locations marked with black arrows.

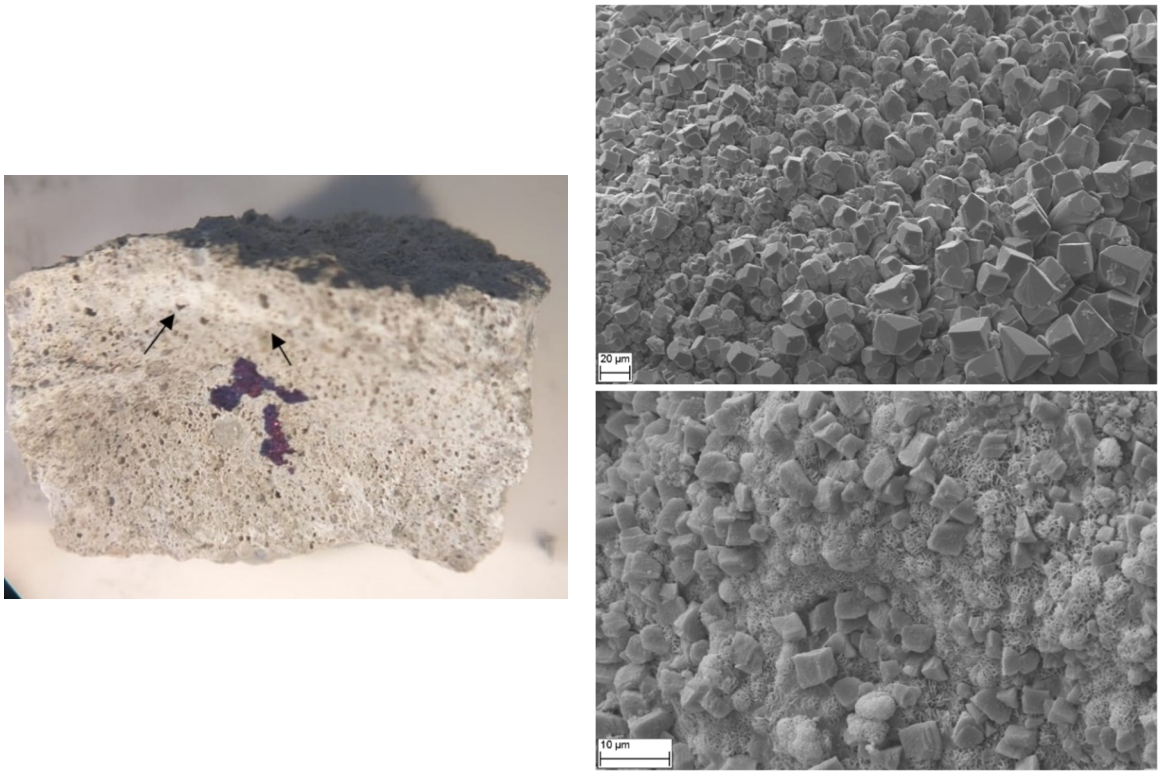

(**a**) (**b**)

Figure 11. (**a**) Exposed crack face of test body with IB3 *Bacillus* sp. and (**b**) SEM image of selected locations marked with black arrows.

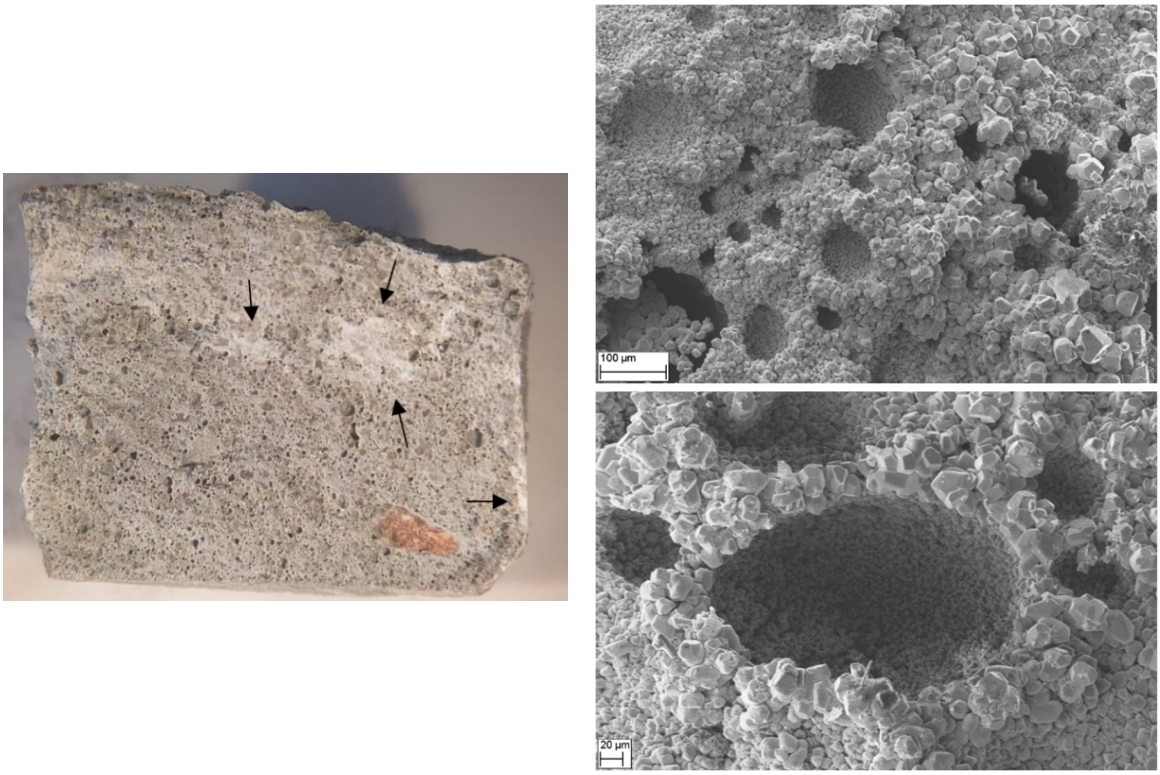

(**a**) (**b**)

Figure 12. (**a**) Exposed crack face of test body with IB4 *Citrobacter* sp. and (**b**) SEM image of selected locations marked with black arrows.

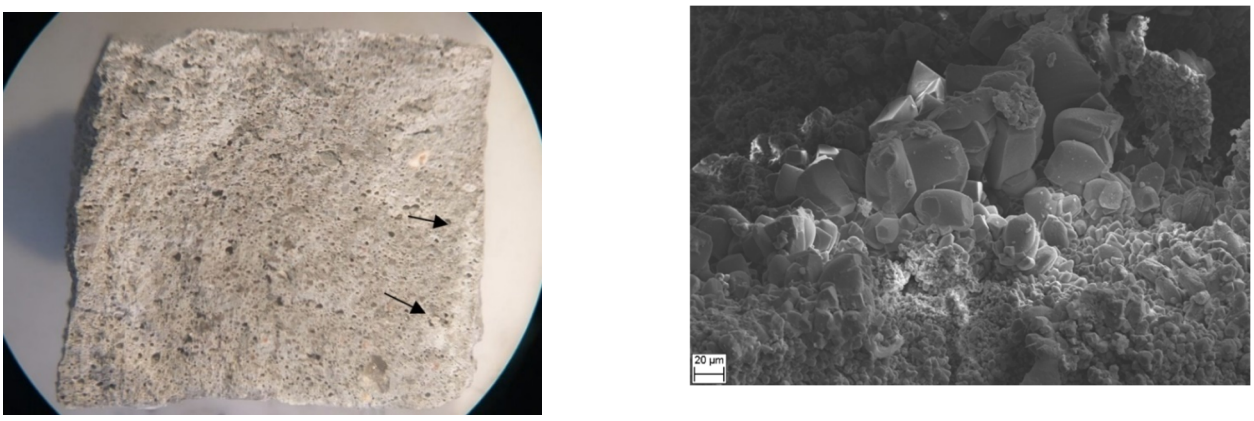

(**a**) (**b**)

Figure 13. (**a**) Exposed crack face of test body with IB5 *Pseudomonas* sp. and (**b**) SEM image of selected locations marked with black arrows.

All SEM images of Figures 9b–13b presented crystal structures with distinct morphologies. Figure 9b shows needle-shaped crystals filling a pore in the cementitious matrix. This was observed in other studies [71] and was attributed to ettringite formation from cement hydration. This phenomenon decreased matrix porosity and increased compaction, which could be viewed as detrimental to the survival of encapsulated bacteria present in the pores. The presence of ettringite in entrained air pores was also observed in samples with IB2 *Cronobacter* sp. This was unsurprising since, as a product of cement hydration, it was likely that the same result should be observed in all other mortars.

Other crystals observed in the SEM images of Figures 9b–13b had rectangular or cubic shapes. These were likely calcium carbonate ($CaCO_3$) as observed in previous studies [24,59,72]. Crystal sizes varied from around 1 µm or less in Figure 10b to between 30 µm and 40 µm in Figures 9b and 13b, although it should be noted that considerable variations in size were commonly noted in the same sample. Other studies have also observed bacterial calcite crystal formations between 1 µm [59] up to around 20 µm [72].

Another formation consisted of crystalized C-S-H superimposed over calcite crystals in a honeycomb shape, as seen in Figures 10b and 12b and also seen in other studies [73,74]. Since C-S-H is a product of cement hydration, it was expected to form before the precipitation of calcite crystals, and its superposition could indicate further hydration of anhydrous cement particles. This superposition could improve calcite adhesion to crack walls but also impede healing since C-S-H would act as a containment barrier to bacteria.

Figure 14 shows XRD diffractograms from materials collected from the cracks. It should be noted that no results were presented from the samples with IB1 *Cronobacter* sp. since no visible healing products were formed or collected.

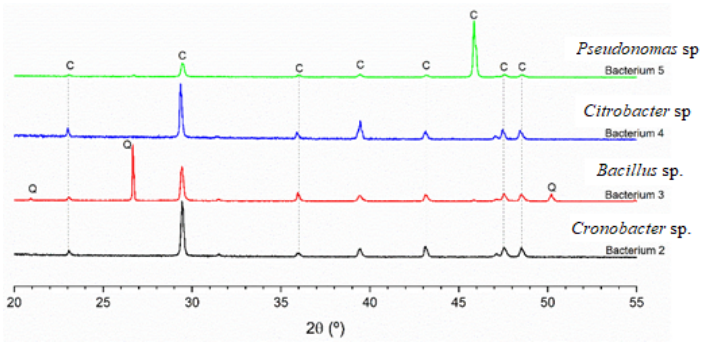

Figure 14. Diffractograms from products collected after 28 days from mortars with IB2 *Cronobacter* sp., IB3 *Bacillus* sp., IB4 *Citrobacter* sp., and IB5 *Pseudonomas* sp. C—calcite and Q—quartz.

Diffractogram results showed that all samples presented characteristic calcite peaks (2θ ≈ 29.5°, 39.5°, and 46°) in their mineral composition. This compound has been observed in other studies [75,76] that utilized bacteria for crack healing, indicating the potential for using indigenous bacteria in cementitious matrices. Additionally, the IB3 *Bacillus* sp. sample also presented characteristic quartz peaks associated with the sand used as light aggregate. This was likely due to contamination when collecting the sample and was also noted in other studies [75].

3.4. Mechanical Compressive Strength

Compressive strength was evaluated at 7 days and 28 days for all five mortar samples and a reference mortar. Results are presented in Figure 15.

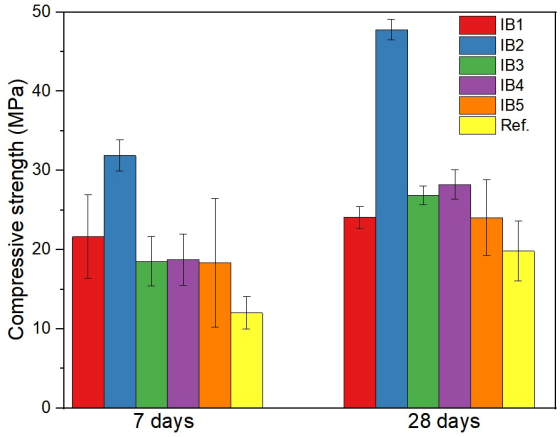

Figure 15. Compressive strength and standard deviation bars at 7 days and 28 days for reference mortar and mortars with IB1 *Cronobacter* sp., IB2 *Cronobacter* sp., IB3 *Bacillus* sp., IB4 *Citrobacter* sp., and IB5 *Pseudomonas* sp.

Figure 15 shows that compressive strength increased for all mortars with bacteria when compared to the reference mortar at both ages. It should be noted that the reference mortar also had entrained air in its matrix and presented an increase in strength of 70% between 7 days and 28 days. This large increase was not observed in the samples incorporating bacteria—the largest increase observed between 7 days and 28 days was 42% for IB2 *Cronobacter* sp. The smaller gain in strength between these ages for mortars incorporating bacteria was likely due to its rise occurring at ages earlier than 7 days. This was indicated from visual analysis that identified healing products being formed at very early ages. Other studies that incorporated bacteria directly into the matrix without encapsulation [47,77–80] also observed increases in strength. This was attributed to MICP in matrix pores decreasing the amount of void spaces and increasing strength. Thus, increases in strength could be taken as a confirmation of bacterial growth in the entrained air pores of the matrix.

At 7 days, the average increase in compressive strength with respect to the reference mortar varied from 57% for IB5 Pseudomonas sp. to 87% for IB1 *Cronobacter* sp. At 28 days, the largest increase in strength with respect to the reference mortar was of 108% for IB2 *Cronobacter* sp. Such a large increase was unreported in other studies and was limited only to IB2 *Cronobacter* sp. for this data set. On the other hand, it should be noted that, due to the large standard deviation bar of IB5 *Pseudomonas* sp., this mortar might have had a similar performance to the reference mortar at 28 days.

Regarding increases in strength for the same mortar between 7 days and 28 days, IB1 *Cronobacter* sp. and IB4 *Citrobacter* sp. presented increases of 10% and 27%, respectively. This agreed with other studies despite differences in mixing technique and bacterium. For

example, adding *B. megaterium* bacteria directly to the mixing water [47] was, in practical terms, similar to encapsulating bacteria in entrained air bubbles but produced a higher increase in strength (24%) in a mortar originally rated at 50 MPa.

Continuing the analysis on the increase in strength between 7 days and 28 days, the reference mortar in this study presented an increase of 9.6 MPa. This indicated that the hydration process was still ongoing and the reference mortar had not reached its maximum strength at 7 days [81]. Consequently, it was to be expected that increases in strength of similar magnitude would be observed in the other mortars. However, the only increase in strength exceeding or approximate to the reference mortar was of 14.5 MPa for IB2 *Cronobacter* sp. This indicated that although bacteria increased the average strength of the mortar, within each type of mortar, they might have had a detrimental effect on the natural cement hydration between 7 days and 28 days.

Some studies reported decreases in compressive strength due to the addition of nutrients in the mortar mix [82]. This was not observed in this study despite calcium lactate and yeast extract being used. On the other hand, the specific use of calcium lactate was also proven to yield a small increase in strength at 28 days [83]. This suggested that the addition of yeast extract might be what affected mortar compressive strength development in this study.

The average increase of 87% in IB1 *Cronobacter* sp. with respect to the reference mortar at 7 days indicated MICP and increased matrix density, and this behavior was also expected to extend to 28 days. However, an amount of stagnation in the increase in strength was observed instead in other mortars. This was likely a result of bacterial activity only at early ages, at which point the local environment was not suitable for their survival. Thus, excess nutrients were left with detrimental effects to strength at later ages. This result pointed to a need for further investigations in this subject.

Results from morphology, mineral composition, and compressive strength are summarized in Table 6 for a comparative analysis.

Table 6. Summary of results of this study

Sample	Soil [1]	Genus	Increase in Compressive Strength (%)			Visual Analysis [2]	SEM and XRD
			7 Days	28 Days			
			With Respect to Reference	With Respire to Reference	With Respect to 7 Days		
IB1	A-II	*Cronobacter*	+87	+10	0	No healing observed	Calcite and ettringite in entrained air pores
IB2	A-V	*Cronobacter*	+147	+108	+42	Crystal formation along the crack at 7 days, growth up to 14 days and reduction at 28 days	Calcite and C-S-H
IB3	B-I	*Bacillus*	+59	+20	+27	Crystal formation along the crack at 14 days and growth up to 28 days	Calcite and C-S-H
IB4	B-II	*Citrobacter*	+72	+28	+26	Crystal formation along the crack at 14 days	Calcite
IB5	B-IV	*Pseudomonas*	+57	+21	+31	Crystal formation along the crack at 14 days and growth up to 28 days	Calcite

[1] Soil samples A-I, A-III, A-IV, B-III, and B-V developed the same bacteria as the ones in this column. Therefore, they were considered duplicates and discarded from the study. [2] Except for the main crack, which did not present any healing in any sample, as discussed in Section 3.2.

4. Conclusions

Bacteria were successfully cultured in a calcium lactate medium and isolated for use in self-healing applications within a cementitious composite. The isolated strains, *Bacillus* (IB3) and *Pseudomonas* (IB5), were previously evaluated in other studies on self-healing concretes.

Microscopic analysis revealed that MICP occurred primarily in recessed regions of the test bodies rather than the top face cracks. The presence of whitish crystals in these areas at 7 days and the loss of healing products over time provided further insight into the dynamic nature of the healing process. Calcium carbonate ($CaCO_3$), identified as the healing product, was consistent with expectations, as the bacteria metabolized the available calcium lactate. The morphological analysis confirmed the presence of calcite crystals with grain sizes ranging from 1 μm to 40 μm.

The inclusion of bacteria in the mortar mixtures resulted in significant increases in compressive strength compared to the reference mortar, with gains of up to 147% at 7 days and 108% at 28 days. Notably, *Cronobacter* sp. IB2 from the Enterobacteriaceae family exhibited the highest improvement, while *Cronobacter* sp. IB1 showed minimal growth, likely due to the presence of residual unconsumed organic nutrients in the matrix.

While this study focused on bacteria isolated from soils in only two Brazilian cities, the findings underscore the importance of exploring additional geographic regions to broaden the understanding of indigenous bacteria for self-healing materials. Furthermore, the successful encapsulation of bacteria in entrained air bubbles using the culture medium as a replacement for mixing water presents a simplified approach for manufacturing self-healing mortars, eliminating the need for additional encapsulating agents.

These results contribute valuable knowledge to the field of self-healing concrete, providing a foundation for future research and development aimed at optimizing the use of indigenous bacteria in cementitious composites.

Author Contributions: Conceptualization, V.M., F.P. and B.F.T.; methodology, V.M., F.P., H.d.S.K. and B.F.T.; formal analysis, V.M., F.P., H.d.S.K., R.C., H.Z.E., V.V., R.C.E.M. and B.F.T.; writing—original draft preparation, V.M., F.P. and H.d.S.K.; writing—review and editing, R.C., H.Z.E., V.V. and R.C.E.M.; supervision, B.F.T. All authors have read and agreed to the published version of the manuscript.

Funding: This research received no external funding.

Institutional Review Board Statement: Not applicable.

Informed Consent Statement: Not applicable.

Data Availability Statement: Dataset available on request from the authors.

Conflicts of Interest: The authors declare no conflict of interest.

References

1. Raza, A.; El Ouni, M.H.; Khan, Q.u.Z.; Azab, M.; Khan, D.; Elhadi, K.M.; Alashker, Y. Sustainability Assessment, Structural Performance and Challenges of Self-Healing Bio-Mineralized Concrete: A Systematic Review for Built Environment Applications. *J. Build. Eng.* **2023**, *66*, 105839. https://doi.org/10.1016/j.jobe.2023.105839.
2. Bagga, M.; Hamley-Bennett, C.; Alex, A.; Freeman, B.L.; Justo-Reinoso, I.; Mihai, I.C.; Gebhard, S.; Paine, K.; Jefferson, A.D.; Masoero, E.; et al. Advancements in Bacteria Based Self-Healing Concrete and the Promise of Modelling. *Constr. Build. Mater.* **2022**, *358*, 129412. https://doi.org/10.1016/j.conbuildmat.2022.129412.
3. Sun, X.; Miao, L.; Wu, L.; Wang, H. Theoretical Quantification for Cracks Repair Based on Microbially Induced Carbonate Precipitation (MICP) Method. *Cem. Concr. Compos.* **2021**, *118*, 103950. https://doi.org/10.1016/j.cemconcomp.2021.103950.

4. Luhar, S.; Luhar, I.; Shaikh, F.U.A. A Review on the Performance Evaluation of Autonomous Self-Healing Bacterial Concrete: Mechanisms, Strength, Durability, and Microstructural Properties. *J. Compos. Sci.* **2022**, *6*, 23. https://doi.org/10.3390/jcs6010023.
5. Benhelal, E.; Zahedi, G.; Shamsaei, E.; Bahadori, A. Global Strategies and Potentials to Curb CO_2 Emissions in Cement Industry. *J. Clean. Prod.* **2013**, *51*, 142–161. https://doi.org/10.1016/j.jclepro.2012.10.049.
6. Hermawan, H.; Minne, P.; Serna, P.; Gruyaert, E. Understanding the Impacts of Healing Agents on the Properties of Fresh and Hardened Self-Healing Concrete: A Review. *Processes* **2021**, *9*, 2206. https://doi.org/10.3390/pr9122206.
7. Qureshi, T.; Al-Tabbaa, A. Self-Healing Concrete and Cementitious Materials. In *Advanced Functional Materials*; Tasaltin, N., Sunday Nnamchi, P., Saud, S., Eds.; IntechOpen: London, UK, 2020; ISBN 978-1-83962-479-7.
8. Amran, M.; Onaizi, A.M.; Fediuk, R.; Vatin, N.I.; Muhammad Rashid, R.S.; Abdelgader, H.; Ozbakkaloglu, T. Self-Healing Concrete as a Prospective Construction Material: A Review. *Materials* **2022**, *15*, 3214. https://doi.org/10.3390/ma15093214.
9. Reinhardt, H.-W.; Jooss, M. Permeability and Self-Healing of Cracked Concrete as a Function of Temperature and Crack Width. *Cem. Concr. Res.* **2003**, *33*, 981–985. https://doi.org/10.1016/S0008-8846(02)01099-2.
10. Nodehi, M.; Ozbakkaloglu, T.; Gholampour, A. A Systematic Review of Bacteria-Based Self-Healing Concrete: Biomineralization, Mechanical, and Durability Properties. *J. Build. Eng.* **2022**, *49*, 104038. https://doi.org/10.1016/j.jobe.2022.104038.
11. Dinarvand, P.; Rashno, A. Review of the Potential Application of Bacteria in Self-Healing and the Improving Properties of Concrete/Mortar. *J. Sustain. Cem.-Based Mater.* **2022**, *11*, 250–271. https://doi.org/10.1080/21650373.2021.1936268.
12. Ahmad, I.; Shokouhian, M.; Jenkins, M.; McLemore, G.L. Quantifying the Self-Healing Efficiency of Bioconcrete Using Bacillus Subtilis Immobilized in Polymer-Coated Lightweight Expanded Clay Aggregates. *Buildings* **2024**, *14*, 3916. https://doi.org/10.3390/buildings14123916.
13. Fahimizadeh, M.; Pasbakhsh, P.; Mae, L.S.; Tan, J.B.L.; Raman, R.K.S. Multifunctional, Sustainable, and Biological Non-Ureolytic Self-Healing Systems for Cement-Based Materials. *Engineering* **2022**, *13*, 217–237. https://doi.org/10.1016/j.eng.2021.11.016.
14. Mello, V.; Pacheco, F.; Tutikian, B.F. Técnicas e Metodologias de Biomineralização Na Cicatrização de Fissuras Do Concreto. *Rev. Arquitetura IMED* **2019**, *8*, 164. https://doi.org/10.18256/2318-1109.2019.v8i2.3679.
15. Achal, V.; Mukerjee, A.; Sudhakara Reddy, M. Biogenic Treatment Improves the Durability and Remediates the Cracks of Concrete Structures. *Constr. Build. Mater.* **2013**, *48*, 1–5. https://doi.org/10.1016/j.conbuildmat.2013.06.061.
16. Rauf, M.; Khaliq, W.; Khushnood, R.A.; Ahmed, I. Comparative Performance of Different Bacteria Immobilized in Natural Fibers for Self-Healing in Concrete. *Constr. Build. Mater.* **2020**, *258*, 119578. https://doi.org/10.1016/j.conbuildmat.2020.119578.
17. Seifan, M.; Samani, A.K.; Berenjian, A. Bioconcrete: Next Generation of Self-Healing Concrete. *Appl. Microbiol. Biotechnol.* **2016**, *100*, 2591–2602. https://doi.org/10.1007/s00253-016-7316-z.
18. Islam, S.U.; Waseem, S.A. Bibliometrics and *Meta* -Analysis of Self-Healing Bio-Concrete—A Systematic Review. *Eur. J. Environ. Civ. Eng*. 2024, *in press*. https://doi.org/10.1080/19648189.2024.2422363.
19. Anbu, P.; Kang, C.-H.; Shin, Y.-J.; So, J.-S. Formations of Calcium Carbonate Minerals by Bacteria and Its Multiple Applications. *SpringerPlus* **2016**, *5*, 250. https://doi.org/10.1186/s40064-016-1869-2.
20. Pacheco, V.L.; Bragagnolo, L.; Reginatto, C.; Thomé, A. Microbially Induced Calcite Precipitation (MICP): Review from an Engineering Perspective. *Geotech. Geol. Eng.* **2022**, *40*, 2379–2396. https://doi.org/10.1007/s10706-021-02041-1.
21. Aytekin, B.; Mardani, A.; Yazıcı, Ş. State-of-Art Review of Bacteria-Based Self-Healing Concrete: Biomineralization Process, Crack Healing, and Mechanical Properties. *Constr. Build. Mater.* **2023**, *378*, 131198. https://doi.org/10.1016/j.conbuildmat.2023.131198.
22. Castro-Alonso, M.J.; Montañez-Hernandez, L.E.; Sanchez-Muñoz, M.A.; Macias Franco, M.R.; Narayanasamy, R.; Balagurusamy, N. Microbially Induced Calcium Carbonate Precipitation (MICP) and Its Potential in Bioconcrete: Microbiological and Molecular Concepts. *Front. Mater.* **2019**, *6*, 126. https://doi.org/10.3389/fmats.2019.00126.
23. Fahimizadeh, M.; Diane Abeyratne, A.; Mae, L.S.; Singh, R.K.R.; Pasbakhsh, P. Biological Self-Healing of Cement Paste and Mortar by Non-Ureolytic Bacteria Encapsulated in Alginate Hydrogel Capsules. *Materials* **2020**, *13*, 3711. https://doi.org/10.3390/ma13173711.
24. Justo-Reinoso, I.; Reeksting, B.J.; Hamley-Bennett, C.; Heath, A.; Gebhard, S.; Paine, K. Air-Entraining Admixtures as a Protection Method for Bacterial Spores in Self-Healing Cementitious Composites: Healing Evaluation of Early and Later-Age Cracks. *Constr. Build. Mater.* **2022**, *327*, 126877. https://doi.org/10.1016/j.conbuildmat.2022.126877.
25. Qu, Z.; Guo, S.; Zheng, Y.; Giakoumatos, E.C.; Yu, Q.; Voets, I.K. A Simple Method to Create Hydrophobic Mortar Using Bacteria Grown in Liquid Cultures. *Constr. Build. Mater.* **2021**, *297*, 123744. https://doi.org/10.1016/j.conbuildmat.2021.123744.
26. Rossi, E.; Raghavan, A.; Copuroglu, O.; Jonkers, H.M. Assessment of Functional Performance, Self-Healing Properties and Degradation Resistance of Poly-Lactic Acid and Polyhydroxyalkanoates Composites. *Polymers* **2022**, *14*, 926. https://doi.org/10.3390/polym14050926.

27. Algaifi, H.A.; Bakar, S.A.; Alyousef, R.; Mohd Sam, A.R.; Ibrahim, M.H.W.; Shahidan, S.; Ibrahim, M.; Salami, B.A. Bio-Inspired Self-Healing of Concrete Cracks Using New B. Pseudomycoides Species. *J. Mater. Res. Technol.* **2021**, *12*, 967–981. https://doi.org/10.1016/j.jmrt.2021.03.037.
28. Chaerun, S.K.; Syarif, R.; Wattimena, R.K. Bacteria Incorporated with Calcium Lactate Pentahydrate to Improve the Mortar Properties and Self-Healing Occurrence. *Sci. Rep.* **2020**, *10*, 17873. https://doi.org/10.1038/s41598-020-74127-4.
29. Joshi, S.; Goyal, S.; Sudhakara Reddy, M. Bio-Consolidation of Cracks with Fly Ash Amended Biogrouting in Concrete Structures. *Constr. Build. Mater.* **2021**, *300*, 124044. https://doi.org/10.1016/j.conbuildmat.2021.124044.
30. Deliktaş, E.B. Investigation of Using Cave Bacteria in the Production of Self-Healing Mortars. *Sigma J. Eng. Nat. Sci.* **2024**, *42*, 1712−1728. https://doi.org/10.14744/sigma.2024.00054.
31. Jonkers, H.M. Bacteria-Based Self-Healing Concrete. *HERON* **2011**, *56*, 49–79.
32. Lee, Y.S.; Park, W. Current Challenges and Future Directions for Bacterial Self-Healing Concrete. *Appl. Microbiol. Biotechnol.* **2018**, *102*, 3059–3070. https://doi.org/10.1007/s00253-018-8830-y.
33. Khaliq, W.; Ehsan, M.B. Crack Healing in Concrete Using Various Bio Influenced Self-Healing Techniques. *Constr. Build. Mater.* **2016**, *102*, 349–357. https://doi.org/10.1016/j.conbuildmat.2015.11.006.
34. Soares, T.V.; Effting, C.; Miranda, K.W.; Schackow, A. Application of Bacterial Nanofibrillated Cellulose for Performance Improvement in Vermiculite Lightweight Mortar. *Constr. Build. Mater.* **2024**, *449*, 138474. https://doi.org/10.1016/j.conbuildmat.2024.138474.
35. Zhang, G.-Z.; Li, S.; Li, H.-F.; Zhang, K.; Cheng, P.-F. Enhancing Self-Healing Performance of Microbial Mortar through Carbon Fiber Reinforcement: An Experimental Analysis. *J. Build. Eng.* **2024**, *91*, 109499. https://doi.org/10.1016/j.jobe.2024.109499.
36. Igbokwe, E.; Ibekwe, S.; Mensah, P.; Agu, O.; Li, G. Self-Healing of Macroscopic Cracks in Concrete by Cellulose Fiber Carried Microbes. *J. Build. Eng.* **2024**, *90*, 109383. https://doi.org/10.1016/j.jobe.2024.109383.
37. Shaheen, N.; Khushnood, R.A.; Khaliq, W.; Murtaza, H.; Iqbal, R.; Khan, M.H. Synthesis and Characterization of Bio-Immobilized Nano/Micro Inert and Reactive Additives for Feasibility Investigation in Self-Healing Concrete. *Constr. Build. Mater.* **2019**, *226*, 492–506. https://doi.org/10.1016/j.conbuildmat.2019.07.202.
38. Xu, H.; Lian, J.; Gao, M.; Fu, D.; Yan, Y. Self-Healing Concrete Using Rubber Particles to Immobilize Bacterial Spores. *Materials* **2019**, *12*, 2313. https://doi.org/10.3390/ma12142313.
39. Lea, F.M.; Hewlett, P.C.; Liska, M. *Lea's Chemistry of Cement and Concrete*; 5th edition.; Butterworth-Heinemann: Oxford, UK; Cambridge, MA, USA, 2019; ISBN 978-0-08-100773-0.
40. Bundur, Z.B.; Amiri, A.; Ersan, Y.C.; Boon, N.; De Belie, N. Impact of Air Entraining Admixtures on Biogenic Calcium Carbonate Precipitation and Bacterial Viability. *Cem. Concr. Res.* **2017**, *98*, 44–49. https://doi.org/10.1016/j.cemconres.2017.04.005.
41. *ASTM C150/C150M-22*; Standard Specification for Portland Cement. American Society for Testing and Materials: West Conshohocken, PA, USA, 2022.
42. Muller, V.; Pacheco, F.; Carvalho, C.M.; Fernandes, F.; Valiati, V.H.; Modolo, R.C.E.; Ehrenbring, H.Z.; Tutikian, B.F. Analysis of Cementitious Matrices Self-Healing with *Bacillus* Bacteria. *Rev. IBRACON Estrut. Mater.* **2022**, *15*, e15404. https://doi.org/10.1590/s1983-41952022000400004.
43. Schwantes-Cezario, N.; Nogueira, G.S.F.; Toralles, B.M. Biocimentação de Compósitos Cimentícios Mediante Adição de Esporos de B. Subtilis AP91. *REC* **2017**, *4*, 142. https://doi.org/10.18256/2358-6508.2017.v4i2.2072.
44. *NBR16887 DE 12/2020*; Concrete—Determination of Air Content in Fresh Concrete—Pressometric Method. Brazilian National Standards Organization: Rio de Janeiro, Brazil, 2020.
45. Algaifi, H.A.; Bakar, S.A.; Sam, A.R.M.; Ismail, M.; Abidin, A.R.Z.; Shahir, S.; Altowayti, W.A.H. Insight into the Role of Microbial Calcium Carbonate and the Factors Involved in Self-Healing Concrete. *Constr. Build. Mater.* **2020**, *254*, 119258. https://doi.org/10.1016/j.conbuildmat.2020.119258.
46. Zhang, J.; Liu, Y.; Feng, T.; Zhou, M.; Zhao, L.; Zhou, A.; Li, Z. Immobilizing Bacteria in Expanded Perlite for the Crack Self-Healing in Concrete. *Constr. Build. Mater.* **2017**, *148*, 610–617. https://doi.org/10.1016/j.conbuildmat.2017.05.021.
47. Andalib, R.; Abd Majid, M.Z.; Hussin, M.W.; Ponraj, M.; Keyvanfar, A.; Mirza, J.; Lee, H.-S. Optimum Concentration of Bacillus Megaterium for Strengthening Structural Concrete. *Constr. Build. Mater.* **2016**, *118*, 180–193. https://doi.org/10.1016/j.conbuildmat.2016.04.142.
48. Madigan, M.T.; Martinko, J.M.; Bender, K.S.; Buckley, D.H.; Stahl, D.A. *Microbiologia de Brock*; 14th ed.; Grupo A Educação S.A.: Porto Alegre, Brazil, 2016.

49. Reche, M.H.L.R.; Reali, C.; Pittol, M.; De Athayde Saul, D.; Macedo, V.R.M.; Valiati, V.H.; Machado, V.; Fiuza, L.M. Diversity of Culturable Gram-Negative Bacteria Isolated from Irrigation Water of Two Rice Crop Regions in Southern Brazil. *Environ. Monit. Assess.* **2016**, *188*, 359. https://doi.org/10.1007/s10661-016-5357-5.
50. Kumar, S.; Stecher, G.; Tamura, K. MEGA7: Molecular Evolutionary Genetics Analysis Version 7.0 for Bigger Datasets. *Mol. Biol. Evol.* **2016**, *33*, 1870–1874. https://doi.org/10.1093/molbev/msw054.
51. Hall, T.A. Bioedit: A User Friendly Biological Sequence Alignment Editor and Analysis Program for Windows 95/98/NT. *Nucleic Acid Symp. Ser.* **1999**, *41*, 95–98.
52. *NBR 7215*; Portland Cement—Determination of Compressive Strength. Brazilian National Standards Organization: Rio de Janeiro, Brazil, 2019.
53. *NBR 13279*; Mortar for Laying and Coating of Walls and Ceilings—Determination of Tensile Strength in Bending and Compression. Brazilian National Standards Organization: Rio de Janeiro, Brazil, 2005.
54. Wang, J.; Dewanckele, J.; Cnudde, V.; Van Vlierberghe, S.; Verstraete, W.; De Belie, N. X-Ray Computed Tomography Proof of Bacterial-Based Self-Healing in Concrete. *Cem. Concr. Compos.* **2014**, *53*, 289–304. https://doi.org/10.1016/j.cemconcomp.2014.07.014.
55. Pacheco, F. Análise Da Eficácia Dos Mecanismos de Autocicatrização Do Concreto. Ph.D. Thesis, University of Vale do Rio dos Sinos Campus : São Leopoldo, Brazil, 2020.
56. Tziviloglou, E.; Wiktor, V.; Jonkers, H.M.; Schlangen, E. Bacteria-Based Self-Healing Concrete to Increase Liquid Tightness of Cracks. *Constr. Build. Mater.* **2016**, *122*, 118–125. https://doi.org/10.1016/j.conbuildmat.2016.06.080.
57. Jenson, I. Bacillus: Introduction. In *Encyclopedia of Food Microbiology*; Elsevier: Amsterdam, The Netherlands, 2010; Volume 1, pp. 111–117.
58. Ehrenbring, H.Z. Desenvolvimento de Engineered Cementitious Composites (ECC) Autocicatrizantes Com Diferentes Fibras Poliméricas e Agentes de Cicatrização. Ph.D. Thesis, University of Vale do Rio dos Sinos Campus : São Leopoldo, Brazil, 2020.
59. Khushnood, R.A.; Arif, A.; Shaheen, N.; Zafar, A.G.; Hassan, T.; Akif, M. Bio-Inspired Self-Healing and Self-Sensing Cementitious Mortar Using Bacillus Subtilis Immobilized on Graphitic Platelets. *Constr. Build. Mater.* **2022**, *316*, 125818. https://doi.org/10.1016/j.conbuildmat.2021.125818.
60. Qian, C.; Rui, Y.; Wang, C.; Wang, X.; Xue, B.; Yi, H. Bio-Mineralization Induced by Bacillus Mucilaginosus in Crack Mouth and Pore Solution of Cement-Based Materials. *Mater. Sci. Eng. C* **2021**, *126*, 112120. https://doi.org/10.1016/j.msec.2021.112120.
61. Nielsen, S.D.; Koren, K.; Löbmann, K.; Hinge, M.; Scoma, A.; Kjeldsen, K.U.; Røy, H. Constraints on $CaCO_3$ Precipitation in Superabsorbent Polymer by Aerobic Bacteria. *Appl. Microbiol. Biotechnol.* **2020**, *104*, 365–375. https://doi.org/10.1007/s00253-019-10215-4.
62. Iglewski, B.H. Pseudomonas. In *Medical Microbiology*; University of Texas Medical Branch: Galveston, TX, USA, 1997.
63. Dodd, C.E.R. Pseudomonas: Introduction. In *Encyclopedia of Food Microbiology*; Elsevier: Amsterdam, The Netherlands, 2014; Volume 3, pp. 244–247.
64. Erşan, Y.Ç.; Hernandez-Sanabria, E.; Boon, N.; De Belie, N. Enhanced Crack Closure Performance of Microbial Mortar through Nitrate Reduction. *Cem. Concr. Compos.* **2016**, *70*, 159–170. https://doi.org/10.1016/j.cemconcomp.2016.04.001.
65. Ramachadran, S.K.; Ramakrishnan, V.; Bang, S.S. Remediation of Concrete Using Microorganisms. *Mater. J.* **2001**, *98*, 3–9. https://doi.org/10.14359/10154.
66. Olstein, A.; Griffith, L.; Feirtag, J.; Pearson, N. Paradigm Diagnostics Salmonella Indicator Broth (PDX-SIB) for Detection of Salmonella on Selected Environmental Surfaces. *J. AOAC INT.* **2013**, *96*, 404–412. https://doi.org/10.5740/jaoacint.11-373.
67. Patel, A.K.; Singhania, R.R.; Pandey, A.; Joshi, V.K.; Nigam, P.S.; Soccol, C.R. *Enterobacteriaceae*, *Coliforms* and *E. Coli*—Introduction. In *Encyclopedia of Food Microbiology*; Elsevier: Amsterdam, The Netherlands, 2014; pp. 659–666; ISBN 978-0-12-384733-1.
68. Koutsoumanis, K.P.; Lianou, A.; Sofos, J.N. Food Safety: Emerging Pathogens. In *Encyclopedia of Agriculture and Food Systems*; Elsevier: Amsterdam, The Netherlands, 2014; Volume 3, pp. 250–272.
69. Zamani, M.; Nikafshar, S.; Mousa, A.; Behnia, A. Bacteria Encapsulation Using Synthesized Polyurea for Self-Healing of Cement Paste. *Constr. Build. Mater.* **2020**, *249*, 118556. https://doi.org/10.1016/j.conbuildmat.2020.118556.
70. Bentz, D.P.; Ardani, A.; Barrett, T.; Jones, S.Z.; Lootens, D.; Peltz, M.A.; Sato, T.; Stutzman, P.E.; Tanesi, J.; Weiss, W.J. Multi-Scale Investigation of the Performance of Limestone in Concrete. *Constr. Build. Mater.* **2015**, *75*, 1–10. https://doi.org/10.1016/j.conbuildmat.2014.10.042.
71. Chichón-Payá, S.; Oliveira, I.; Aguado, A.; Chinchón-Yepes, S. The Sulfate Attack in Concrete by Degradation of Iron Sulfides and the Effect of the Host Rock. Presented at the II DBMC. In Proceedings of the International Conference on Durability of Building Materials and Components, Porto, Portugal, 12 April 2011.

72. Wang, J.; Mignon, A.; Trenson, G.; Van Vlierberghe, S.; Boon, N.; De Belie, N. A Chitosan Based pH-Responsive Hydrogel for Encapsulation of Bacteria for Self-Sealing Concrete. *Cem. Concr. Compos.* **2018**, *93*, 309–322. https://doi.org/10.1016/j.cemconcomp.2018.08.007.
73. Borštnar, M.; Daneu, N.; Dolenec, S. Phase Development and Hydration Kinetics of Belite-Calcium Sulfoaluminate Cements at Different Curing Temperatures. *Ceram. Int.* **2020**, *46*, 29421–29428. https://doi.org/10.1016/j.ceramint.2020.05.029.
74. Kunal; Siddique, R.; Rajor, A.; Singh, M. Influence of Bacterial-Treated Cement Kiln Dust on Strength and Permeability of Concrete. *J. Mater. Civ. Eng.* **2016**, *28*, 04016088. https://doi.org/10.1061/(ASCE)MT.1943-5533.0001593.
75. Xu, J.; Wang, X.; Wang, B. Biochemical Process of Ureolysis-Based Microbial $CaCO_3$ Precipitation and Its Application in Self-Healing Concrete. *Appl. Microbiol. Biotechnol.* **2018**, *102*, 3121–3132. https://doi.org/10.1007/s00253-018-8779-x.
76. Yuan, H.; Zhang, Q.; Hu, X.; Wu, M.; Zhao, Y.; Feng, Y.; Shen, D. Application of Zeolite as a Bacterial Carrier in the Self-Healing of Cement Mortar Cracks. *Constr. Build. Mater.* **2022**, *331*, 127324. https://doi.org/10.1016/j.conbuildmat.2022.127324.
77. Qian, C.; Ren, L.; Xue, B.; Cao, T. Bio-Mineralization on Cement-Based Materials Consuming CO_2 from Atmosphere. *Constr. Build. Mater.* **2016**, *106*, 126–132. https://doi.org/10.1016/j.conbuildmat.2015.10.105.
78. Siddique, R.; Nanda, V.; Kunal; Kadri, E.-H.; Iqbal Khan, M.; Singh, M.; Rajor, A. Influence of Bacteria on Compressive Strength and Permeation Properties of Concrete Made with Cement Baghouse Filter Dust. *Constr. Build. Mater.* **2016**, *106*, 461–469. https://doi.org/10.1016/j.conbuildmat.2015.12.112.
79. Siddique, R.; Singh, K.; Kunal; Singh, M.; Corinaldesi, V.; Rajor, A. Properties of Bacterial Rice Husk Ash Concrete. *Constr. Build. Mater.* **2016**, *121*, 112–119. https://doi.org/10.1016/j.conbuildmat.2016.05.146.
80. Siddique, R.; Jameel, A.; Singh, M.; Barnat-Hunek, D.; Kunal; Aït-Mokhtar, A.; Belarbi, R.; Rajor, A. Effect of Bacteria on Strength, Permeation Characteristics and Micro-Structure of Silica Fume Concrete. *Constr. Build. Mater.* **2017**, *142*, 92–100. https://doi.org/10.1016/j.conbuildmat.2017.03.057.
81. Lothenbach, B.; Le Saout, G.; Gallucci, E.; Scrivener, K. Influence of Limestone on the Hydration of Portland Cements. *Cem. Concr. Res.* **2008**, *38*, 848–860. https://doi.org/10.1016/j.cemconres.2008.01.002.
82. Jang, I.; Son, D.; Kim, W.; Park, W.; Yi, C. Effects of Spray-Dried Co-Cultured Bacteria on Cement Mortar. *Constr. Build. Mater.* **2020**, *243*, 118206. https://doi.org/10.1016/j.conbuildmat.2020.118206.
83. Luo, M.; Qian, C. Influences of Bacteria-Based Self-Healing Agents on Cementitious Materials Hydration Kinetics and Compressive Strength. *Constr. Build. Mater.* **2016**, *121*, 659–663. https://doi.org/10.1016/j.conbuildmat.2016.06.075.